



## Transportmetrica A: Transport Science

Publication details, including instructions for authors and subscription information:

<http://www.tandfonline.com/loi/ttra21>

### Characterisation of driver behaviour during car following using quantum optical flow theory

Jiuh-Biing Sheu <sup>a</sup>

<sup>a</sup> Institute of Traffic and Transportation, National Chiao Tung University , 4F, 118 Chung Hsiao W. Rd., Sec. 1, Taipei , 10012 , Taiwan , ROC

Published online: 12 May 2011.

To cite this article: Jiuh-Biing Sheu (2013) Characterisation of driver behaviour during car following using quantum optical flow theory, *Transportmetrica A: Transport Science*, 9:3, 269-298, DOI:

[10.1080/18128602.2011.572571](http://10.1080/18128602.2011.572571)

To link to this article: <http://dx.doi.org/10.1080/18128602.2011.572571>

PLEASE SCROLL DOWN FOR ARTICLE

Taylor & Francis makes every effort to ensure the accuracy of all the information (the "Content") contained in the publications on our platform. However, Taylor & Francis, our agents, and our licensors make no representations or warranties whatsoever as to the accuracy, completeness, or suitability for any purpose of the Content. Any opinions and views expressed in this publication are the opinions and views of the authors, and are not the views of or endorsed by Taylor & Francis. The accuracy of the Content should not be relied upon and should be independently verified with primary sources of information. Taylor and Francis shall not be liable for any losses, actions, claims, proceedings, demands, costs, expenses, damages, and other liabilities whatsoever or howsoever caused arising directly or indirectly in connection with, in relation to or arising out of the use of the Content.

This article may be used for research, teaching, and private study purposes. Any substantial or systematic reproduction, redistribution, reselling, loan, sub-licensing, systematic supply, or distribution in any form to anyone is expressly forbidden. Terms & Conditions of access and use can be found at <http://www.tandfonline.com/page/terms-and-conditions>

## Characterisation of driver behaviour during car following using quantum optical flow theory

Jiuh-Biing Sheu\*

*Institute of Traffic and Transportation, National Chiao Tung University,  
4F, 118 Chung Hsiao W. Rd., Sec. 1, Taipei 10012, Taiwan, ROC*

*(Received 18 March 2010; final version received 12 March 2011)*

This study characterises driver behaviour during car following using a quantum optical-flow-based model. Car following is deemed the outcome of the intuitive response of a driver to instantaneous optical stimuli in the visual field driven by changes in the surrounding traffic environments. Such optical stimuli are transformed into psychophysical momentums in the quantum optical field using quantum mechanics, and then used to approximate the driver speed adjustment in the optical-flow-induced stimulus-response process. Preliminary test results using video-based data reveal the potential of the proposed model's applicability in characterising driver decisions to adjust speed in response to changes in surrounding traffic situations perceived in the visual field. Generalisations of analytical results also infer that under a plausible condition that a following driver fully focused on the front vehicle's behaviour, the proposed model permits reproducing car-following behaviour similar to that generated by existing models.

**Keywords:** quantum mechanics; optical flow; driver behaviour; car-following models

### 1. Introduction

Car-following behaviour which characterises driver responses to speed changes by the front vehicle without lane changes in a lane traffic stream have been extensively investigated using numerous microscopic traffic behaviour models. Typical among these include linear models (Pipes 1953, Chandler *et al.* 1958, Herman and Rothery 1965), nonlinear approximations (Gazis *et al.* 1961, Newell 1961), and the incorporation of artificial inference (AI) techniques such as fuzzy theories (Kikuchi and Chakroborty 1992, Chakroborty and Kikuchi 1999). Additionally, remarkable improvements in addressing diverse car-following phenomena, e.g. reaction time delay (Davis 2003, Orosz *et al.* 2005), night driving (Jiang and Wu 2007) and asymmetrical full velocity difference of vehicles in a traffic stream (Gong *et al.* 2008) have recently been made. Brackstone and McDonald (1999) conducted an in-depth review of car-following theories, and identified the following five major groups of car-following models: (1) the Gazis–Herman–Rothery (GHR) model; (2) safety distance or collision avoidance (CA) models; (3) Helly-based linear models; (4) psychophysical or action point (AP) models and (5) fuzzy-logic-based models.

---

\*Email: [jbsheu@mail.nctu.edu.tw](mailto:jbsheu@mail.nctu.edu.tw)

Briefly, existing car-following models assume that movement of a following vehicle is influenced primarily by the front vehicle, and the following vehicle adjusts its speed based on the relative speed and distance of the front vehicle.

Despite the considerable advances in car-following theories, the characterisation of the following lane traffic phenomena leaves space for discussion. First, let us consider a case in which an incident occurs in an adjacent lane, and is perceived by the driver of a target vehicle; meanwhile, another vehicle is moving ahead in the same lane as the target vehicle. Intuitively, the target driver does not react only to the behaviour of the front vehicle when passing the incident. Rather, the incident may affect the behaviour of the target driver, contributing to a rubbernecking effect during car-following manoeuvres (Sheu 2008). Second, consider the case in which only one front vehicle is moving ahead of the target vehicle in a given lane. Given the same initial traffic conditions, including the gap and relative speeds of these two vehicles, different front vehicles may cause different car-following manoeuvres by the target vehicle. For example, the response of the target driver to a truck ahead during car following may differ significantly from that when responding to a typical automobile. Additionally, under heavy traffic congestion, some drivers may take the risk of following the front vehicle with an extremely short gap to prevent vehicles in adjacent lanes from entering the gap immediately in front of their vehicles (Ranney 1999). This also complicates the reproduction of intra-lane traffic behaviour using classical car-following models if only the longitudinal relationship between the following and front vehicles is taken into account.

Furthermore, consensus exists among traffic engineers that a traffic system consists of three elements: (1) road users; (2) vehicles and (3) infrastructure. These elements contribute to diverse traffic phenomena. Unfortunately, most traffic phenomena cannot be characterised by pure physics and fluid theories without considering human factors, external environments and the complex stimulus-response process among these elements that vary over time and space. Particularly, microscopic traffic behaviour models such as car-following theories should not be limited to reproducing specific 'traffic-particle' locomotion using classical physical theorems; rather, such human factors as driver perception of moving entities and the resulting psychological and physiological stimuli should be considered to rationalise the causes and effects of 'real' driver behaviour during car following. One noticeable example is the developmental tendency of advanced microscopic traffic simulators which incorporate more psychophysical thresholds and functions into microscopic traffic simulation to reproduce sophisticated car-following behaviour in response to diverse traffic flow phenomena (Wiedemann 1991, Fritzsche 1994, Panwai and Dia 2005, Tampere *et al.* 2009).

Thus, this work characterises the dynamic decision process, including the causes and effects of individual driver behaviour when moving in a given lane, using a quantum optical-flow-based driver stimulus-response model. For the sake of simplicity, the proposed model does not consider the influence of other traffic information sources, such as traffic signals and variable message signs (VMSs), on driver behaviour. However, this work does account for several physical and psychological factors during model formulation such as the stimulus from variations in optical flows and the size of driver attentional resources. The initial stimulus from perceived changes in front traffic and geometric situations is first transformed into psychological stimuli (i.e. psychophysical momentums) using a quantum-mechanics-based approach. The estimated psychophysical momentums are then used to approximate the resulting speed adjustment of a driver.

This work adopts the underlying concepts of computational judgement theories (Fodor 1983, MacLeod and Ross 1983, Cavallo and Laurent 1988, Baker 1999) rather than those of ecological optical theories (Gibson 1966, Lee 1980) to deal with the aforementioned visual stimuli transformation in the quantum optical field. As noted by Baker (1999), relative to ecological optical approaches that assume information is directly available from a user's optical array and immediately usable without further transformation, computational judgement theories posit that complex mental calculations are needed to process visual stimuli from moving images into behavioural outcomes. Thus, judgement errors may occur while perceiving moving images due to the wave–image duality during the transfer of visual information; thus, an uncertain relationship exists between the perception of speed and the focal point of the quantum optical field. Consequently, the quantum optical flow approach is utilised to characterise the dynamic and uncertain properties of driver perception of moving environments while moving in a given lane without considering lane-changing manoeuvres.

Moreover, the rationalisation of driver behaviour addressed by the proposed model is rooted in the belief that driver's vision is the key interface between external stimuli and driving responses. Unlike the idealistic car-following logic that the speed adjustment of a target driver in a lane is primarily based on the relative relationship between two successive vehicles moving in the same lane, the proposed model assumes that all perceived objects, including front vehicles moving in the same lane or adjacent lanes, affect target driver decisions. Using quantum optical flow theories, such effects are transmitted as quantum-based psychophysical momentums, thereby stimulating intuitive speed adjustment by a driver. Furthermore, driver intra-lane speed adjustment is considered as the accommodative response resulting intuitively from optical stimuli rather than as a consensual output between leading and following vehicles.

Relative to the previous literature in quantum optical flow theory, the incremental contribution of this work can also be highlighted in two aspects: (1) model extension to provide a link that bridges the gap between quantum optical flow and car-following theories and (2) model tests through experimental design and video-based data to demonstrate the applicability of the proposed model in diverse traffic flow conditions. As to model extension, the proposed model not only characterises the quantum uncertainty relationship between the quantum optical field and a driver's speed perception, but also transforms visual stimuli into psychological stimuli so as to approximate the driver's speed adjustment in a car-following process. With respect to model tests, this work adopts two test scenarios using different video-based datasets collected at an urban highway of Taiwan and a freeway of California to not only enrich the variety of data acquisition but also demonstrate the transferability of the proposed model. These are detailed in Sections 2 and 3, respectively.

## 2. Modelling

Consider a target vehicle moving in a given lane on a roadway without attempting to change lanes, and not influenced by external information sources such as traffic signals and message signs. This work argues that perceived objects (e.g. vehicles) moving on the roadway are the major source of visual stimuli impacting the speed adjustment of the target-vehicle driver during the car-following process. Thus, this work develops a novel

stimulus–response driver behaviour model using a quantum-mechanics-based approach. The proposed model consists of the following two recursive phases: (1) transformation of visual stimuli and (2) approximation of speed adjustment. A quantum optical flow approach is applied in phase 1 to characterise perceived surrounding traffic flow conditions transformed from visual stimuli into psychological stimuli (called psychophysical momentum in this work). The developed quantum-mechanics-based driver–response model then approximates driver speed adjustment in response to visual stimuli in phase 2. Figure 1 shows the entire conceptual framework of the proposed model. The details regarding model formulation are described as follows.

### 2.1. Quantum transformation of visual stimuli

This phase models driver visual stimuli (i.e. driver-perceived traffic flow conditions) using quantum optical flow theory that transforms visual stimuli into psychological stimuli (i.e. psychophysical momentum). Quantum optical flow theory can be considered an extension of a cognitive approach (MacLeod and Ross 1983, Cavallo and Laurent 1988, Baker 1999), and is an alternative method for characterising the impact of optical flow on individual decisions, relative to ecological optical theories (Gibson 1966, Lee 1980). According to Baker (1999), the quantum mechanism approach is particularly applicable for explaining motion-related perceptual phenomena, including the visual cause-and-effect of motion and high-speed adaptation. Sheu (2008) applied such a quantum-mechanics-based theory to explicate how a driver is affected by lane-blocking incidents in adjacent lanes when approaching an incident site. Motivated by these studies, this work adopts quantum optical flow theory to develop a transformation function that conceptualises

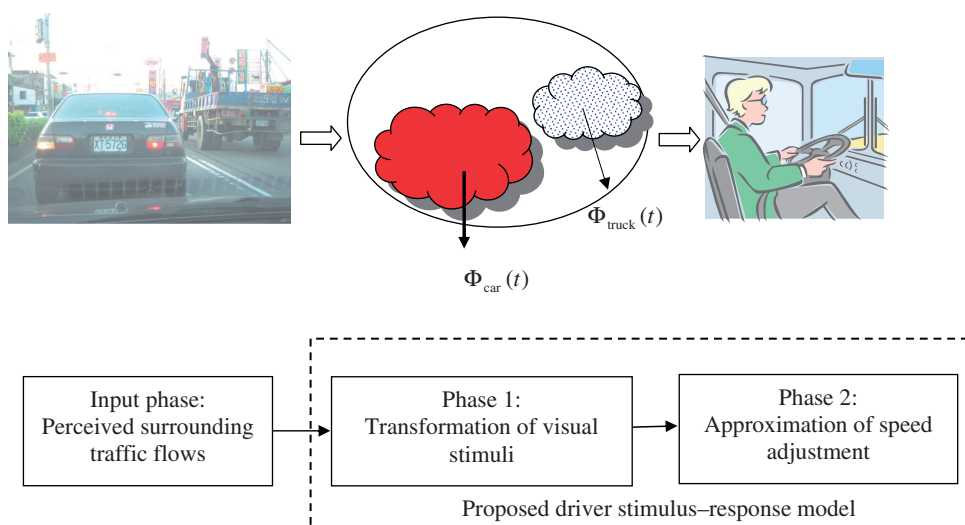


Figure 1. Conceptual framework of the proposed model.

visual stimuli perceived by a target driver in the quantum optical field. The developmental process is as follows.

First, target vehicle  $i$  moves in a given lane  $l$  at time  $t$ . According to quantum optical flow theories (Miura 1987, Osaka 1988, Bartmann *et al.* 1991, Kayser and Hess 1991, Baker 1999), one can define a quantum optical field ( $Q[\Delta x(t), \Delta y(t)]$ ) associated with the target driver to characterise the probability-related allocation range (i.e.  $\Delta x(t)$  and  $\Delta y(t)$ ) of target driver attention across the longitudinal ( $X$ ) and lateral ( $Y$ ) dimensions of  $Q[\Delta x(t), \Delta y(t)]$ ; thus, we have

$$(\Delta x(t))(v_i(t)) = C_X, \quad \forall t \quad (1)$$

$$(\Delta y(t))(v_i(t)) = C_Y, \quad \forall t \quad (2)$$

where  $\Delta x(t)$  and  $\Delta y(t)$  are the standard deviation in the longitudinal ( $X$ ) and lateral ( $Y$ ) dimensions of the focal point of the target driver, respectively;  $v_i(t)$  is the instantaneous speed of target vehicle  $i$  moving along the  $X$ -dimension at time  $t$  and  $C_X$  and  $C_Y$  are two constants associated with the  $X$ - and  $Y$ -dimensions, respectively. In reality, the original forms of Equations (1) and (2) were proposed in Baker (1999) to characterise the relationships between the uncertainties ( $\Delta x$  and  $\Delta y$ ) in the two-dimensional focal point of a driver and driving speed ( $v$ ). Experimental studies to support Equations (1) and (2) can be found in Bartmann *et al.* (1991) and Kayser and Hess (1991). Here, the uncertainties in a quantum optical field ( $Q[\Delta x(t), \Delta y(t)]$ ) change as  $v_i(t)$  changes. As argued by Baker (1999), a high vehicular speed requires concentration to process resources, thus forming what is called driver ‘tunnel vision’, which is a manifestation of a focus on forward motion. Conversely, a low vehicular speed may result in the increases in  $\Delta x$  and  $\Delta y$ , leading to more uncertainties in  $Q[\Delta x(t), \Delta y(t)]$  of a driver. Therefore, a trade-off relationship may exist between  $\Delta y(t)$  and  $v_i(t)$ , as in Equation (2), and a similar trade-off also applies to the relationship between  $\Delta x(t)$  and  $v_i(t)$ , as in Equation (1).

Nevertheless, the aforementioned relationship between  $Q[\Delta x(t), \Delta y(t)]$  and  $v_i(t)$  also hinges on an inequality and factors such as driver attentional resources and an action constant. Such uncertainty underpins the mistakes that a driver can make in driving judgement especially with speed (Baker 1999), which is further detailed in the rest of this section. Furthermore, Miura (1987) had confirmed that the relationship of aerial uncertainties (of the fovea) in  $Q[\Delta x(t), \Delta y(t)]$  may exist in the form as  $[\Delta x(t)][\Delta y(t)] \approx C_{XY}$ , which means that there is also a trade-off between  $\Delta x(t)$  and  $\Delta y$  in a quantum optical field, where  $C_{XY}$  is a constant. Therefore, given that vehicular speed ( $v_i(t)$ ) remains constant, the uncertainty in the lateral optical field decreases as the uncertainty in the longitudinal optical field increases.

Suppose the target driver observes surrounding traffic flows composed of a certain number of vehicles ahead (denoted by  $J_Q$ ) within the corresponding quantum optical field ( $Q[\Delta x(t), \Delta y(t)]$ ) at time  $t$ . Via the effect of optical flow, each perceived vehicle  $j_Q$  then contributes to the instantaneous psychophysical momentum ( $\Phi_{j_Q}(t)$ ) and the psychophysical energy function ( $\theta_{j_Q}(t)$ ) of the target driver; thus,  $\Phi_{j_Q}(t)$  and  $\theta_{j_Q}(t)$  are given by

$$\Phi_{j_Q}(t) = m_{j_Q} \times v_{j_Q \rightarrow i}(t) \times W_i(t), \quad \forall j_Q \in J_Q \quad (3)$$

$$\theta_{j_Q}(t) = \frac{m_{j_Q} \times [v_{j_Q \rightarrow i}(t)]^2 \times W_i(t)}{2}, \quad \forall j_Q \in J_Q \quad (4)$$

where  $j_Q$  is a given nearby vehicle perceived by a target driver within  $Q[\Delta x(t), \Delta y(t)]$  at time  $t$ ;  $m_{j_Q}$  is the perceived light mass associated with  $j_Q$ ;  $v_{j_Q \rightarrow i}(t)$  is the perceived relative speed of  $j_Q$  with respect to target vehicle  $i$  at time  $t$ , which is given by  $v_{j_Q \rightarrow i}(t) = v_{j_Q}(t) - v_i(t)$ ;  $W_i(t)$  is defined as the size of attentional resources associated with target driver  $i$  at time  $t$ , based on attention theory in psychology (Kahneman 1973, Hasher and Zacks 1979, Humphreys and Revelle 1984, Eriksen and St James 1986, Young and Stanton 2002). Our rationales for the definition of  $W_i(t)$  are summarised as follows. According to Kahneman (1973), attentional capacity determined by attentional resources is positively associated with physiological arousal. Furthermore, the size of attentional resources may change not only with long-term fluctuation in mood or age (Hasher and Zacks 1979, Humphreys and Revelle 1984) but also in the relatively short term depending on task conditions (Young and Stanton 2002). If attentional resources are fixed, the larger the optical field is, the slower the processing will be in the optical field, according to the zoom-lens model in the field of selective visual attention (Eriksen and St James 1986). Additionally, it is noteworthy that the current study scope including the proposed model aims at urban rather than rural roads and that the light mass perceived is restricted to the case of day trips rather than night trips which can be influenced by other factors such as environmental lightness including the performance of vehicular headlights and perceived brake lights. A driver with a higher value of  $W_i(t)$  may perceive a greater psychophysical momentum (Sheu 2008). According to Equation (3), a negative psychophysical momentum ( $\Phi_{j_Q}(t) < 0$ ) may occur in the case  $v_{j_Q \rightarrow i}(t) < 0$ , meaning that the physical speed of the perceived surrounding vehicle  $j_Q$  is lower than that of the target vehicle  $i$ . This may lead to the target driver's visual phenomenon that the perceived surrounding vehicle  $j_Q$  is moving backward (i.e. towards the target driver). In this work, such a negative psychophysical momentum ( $\Phi_{j_Q}(t) < 0$ ) is regarded as a negative stimulus to the target driver, and thus it may cause a negative effect on the speed adjustment (i.e. deceleration) of the target driver. Nevertheless, the magnitude of this effect also depends on the size of a driver's attentional resources ( $W_i(t)$ ). A driver with a high value of  $W_i(t)$  may perceive a greater negative psychophysical momentum than a driver with a low value of  $W_i(t)$  under the condition of  $v_{j_Q \rightarrow i}(t) < 0$ . This is one reason why  $W_i(t)$  is incorporated into the above model formulation.

Nevertheless, psychophysical energy, according to Baker (1999), must be defined as a function of optical flow frequency and follow the stability rules of the quantum solution. Thus, by employing classical quantum equations, the following conditions that characterise the correlations between the waveform of a visual stimulus (i.e. perceived vehicular image) and psychological stimulus (i.e. psychophysical momentum and energy function) also hold for each vehicle  $j_Q$  perceived within the quantum optical field.

$$\Phi_{j_Q}(t) = \frac{h}{\omega_{j_Q}(t)}, \quad \forall j_Q \in J_Q \quad (5)$$

$$\theta_{j_Q}(t) = h \times f_{j_Q}(t), \quad \forall j_Q \in J_Q \quad (6)$$

where  $\omega_{j_Q}(t)$  and  $f_{j_Q}(t)$  are the wavelength and frequency associated with the quantum optical flow oriented from  $j_Q$  perceived by target driver at time  $t$ , respectively, and  $h$  is an

action constant. Similarly, the perceived image associated with  $j_Q$  can be characterised as a waveform with wavelength ( $\omega_{j_Q}(t)$ ) and frequency ( $f_{j_Q}(t)$ ), and is given by

$$\omega_{j_Q}(t) = \frac{h}{\Phi_{j_Q}(t)}, \quad \forall j_Q \in J_Q \quad (7)$$

$$f_{j_Q}(t) = \frac{\theta_{j_Q}(t)}{h}, \quad \forall j_Q \in J_Q \quad (8)$$

Using Equations (3), (4), (7) and (8) combined with the theory of wave packet formation, this work approximates the wavelength ( $\omega_{J_Q}(t)$ ) of the wave packet caused by perceived surrounding traffic flows ( $J_Q$ ), and the propagation coefficient ( $p(t)$ ) from the wave modulation subject to the following condition:

$$\omega_{J_Q}(t) = \frac{2\pi}{p(t)} = \frac{4\pi}{\Delta p(t)} \quad (9)$$

where  $p(t) = \frac{\Delta p(t)}{2}$ . Based on the image–wave duality relationship obtained by combining Equations (7)–(9), we have

$$\omega_{J_Q}(t) = \frac{h}{\Phi_{J_Q}(t)} \quad (10)$$

$$p(t) = \frac{2\pi\Phi_{J_Q}(t)}{h} \quad (11)$$

where  $\Phi_{J_Q}(t)$  is the aggregate psychophysical momentum caused by perceived surrounding traffic flows, and is described in the following subsection. According to Beiser (1969), Morrison (1990) and Baker (1999), the resulting wave packet spread ( $\Delta x(t)$ ) is best defined by  $\Delta x(t) = \frac{2\pi}{\Delta p(t)} = \frac{\omega_{J_Q}(t)}{2}$ . Thus,  $\Delta x(t)$  also represents the instantaneous visual scope in the longitudinal dimension of the quantum optical field at time  $t$ , as described previously. Accordingly, the uncertainty ( $\Delta\Phi_{J_Q}(t)$ ) in the psychophysical momentum caused by the perceived surrounding traffic flows can be defined as

$$\Delta\Phi_{J_Q}(t) = \frac{h\Delta p(t)}{2\pi} = \frac{h}{\Delta x(t)} \quad (12)$$

Generally, Equation (12) can be expressed in the form of the Heisenberg Uncertainty Principle given by

$$\Delta x(t)\Delta\Phi_{J_Q}(t) \geq h \quad (13)$$

Equation (13) indicates that the joint uncertainty in the longitudinal field of the driver's focal point ( $\Delta x$ ) and psychophysical momentum ( $\Delta\Phi_{J_Q}(t)$ ) is greater and equal to an action constant ( $h$ ). However, according to Equation (10), the lower the perceived relative speed ( $v_{J_Q \rightarrow i}(t)$ ), the longer the wavelength ( $\omega_{J_Q}(t)$ ) in seeing the surrounding traffic flows ( $M_{J_Q}$ ) and the greater the value of  $\Delta x$  ( $\therefore \Delta x(t) = \frac{\omega_{J_Q}(t)}{2}$ ), leading to lower uncertainty in

psychophysical momentum ( $\Delta\Phi_{J_Q}(t)$ ). Given that the size of the target driver's attentional resources ( $W_i(t)$ ) is constant at time  $t$ , we can then rewrite Equation (13) as

$$\Delta x(t)\Delta v_{J_Q \rightarrow i}(t) \geq \frac{h}{M_{J_Q} \times W_i(t)} \quad (14)$$

where the sign  $\geq$  is a formal statistical statement relating the standard deviations in longitudinal field ( $\Delta x(t)$ ) and speed perception ( $\Delta v_{J_Q \rightarrow i}(t)$ ) with a workload constant ( $\frac{h}{M_{J_Q} W_i(t)}$ ) that can be multiples of the wave packets of the perceived images from relative motion. In this work, we define the entire right hand side of  $\geq$  as a mental workload constant based on Wickens and Hollands (2000) and Patten *et al.* (2004) that address driver attention allocation. In Wickens and Hollands (2000), the workload of a driver is defined as the demand of driver mental resources allocated per time unit for driving performance. Patten *et al.* (2004) further claimed that driver mental workload is associated negatively with a driver's awareness of road situations. In Baker (1999) such an inequality sign represents that the wave packet may have different shapes apart from a normal distribution. Accordingly, Equation (14) indicates that for a driver with fixed attentional resources for a while ( $W_i(t)$  is constant), the greater the uncertainty in the driver's focal point, the smaller the errors in the driver's judgement of relative speed with respect to the perceived surrounding vehicles, and *vice versa*.

Note that the right-hand side of  $\geq$  shown in Equation (14) is regarded as a mental workload factor associated with a driver, and embeds the attentional-resource term ( $W_i(t)$ ) that describes the internal characteristics of the driver. If  $W_i(t)$  is assumed to be complex with real and imaginary components, the right-hand side of  $\geq$  shown in Equation (14) can then be written in the complex form of  $\frac{ih}{2\pi}$ . Correspondingly, the uncertainties in driver perception for both the longitudinal ( $X$ ) and lateral ( $Y$ ) dimensions and speed can then be described, respectively, as

$$[\Delta x(t)][\Delta v_{J_Q \rightarrow i}(t)] \geq \frac{ih}{2\pi M_{J_Q} W_i(t)} \text{ for longitudinal field,} \quad (15)$$

$$[\Delta y(t)][\Delta v_{J_Q \rightarrow i}(t)] \geq \frac{ih}{2\pi M_{J_Q} W_i(t)} \text{ for lateral field.} \quad (16)$$

Note that both Equations (15) and (16) follow the Heisenberg Uncertainty Principle, and the right-hand side ( $\frac{ih}{2\pi M_{J_Q} W_i(t)}$ ) of the sign  $\geq$  remains as a complex workload constant. According to Baker (1999), Equations (15) and (16) can also be expressed as a combinative form given by

$$[\Delta x(t)\Delta y(t)][\Delta v_{J_Q \rightarrow i}(t)]^2 \geq -\frac{h^2}{4\pi^2 (M_{J_Q})^2 [W_i(t)]^2} \quad (17)$$

Therein, Equation (17) can be regarded as a generalised form of the proposed model used to characterise the trade-off relationship between the joint uncertainty in a quantum optical field  $[\Delta x(t) \Delta y(t)]$  and the standard deviation ( $\Delta v_{J_Q \rightarrow i}(t)$ ) in a driver's speed perception constrained by a complex workload constant. In other words, the simultaneous measurement of a driver's perceived relative speed and the instantaneous visual spread entails a limitation on the precision (standard deviation) of each measurement. The more

precise the measurement of a driver's perceived relative speed, the more imprecise the measurement of instantaneous visual spread, and vice versa. In the most extreme case, absolute precision of one variable would entail absolute imprecision regarding the other. Because of the nature of light within the optic flow that human beings have to process to obtain visualisation, errors may occur within the computation judgement of motion relative to speed.

Despite the rationality of quantum mechanics approaches applied in the analysis of optical flow, the purpose of the proposed model is to reproduce a driver's car-following behaviour for day trips on urban roadways rather than the quantum movement of a tiny particle (e.g. an electron) with unlimited measurement errors in either position or momentum. Therein, we are more interested in a constrained speed-perception error case  $[\Delta v_{J_Q \rightarrow i}(t)] \rightarrow [v_{J_Q \rightarrow i}(t)]$  meaning that a driver perceives the speed of the optic flow as physical speed with no deviation in estimation. Under such a prerequisite, we can then readily describe the quantum optical flow of a driver as looking at variations in the likelihood of spatial field perception relative to other surrounding vehicle movements. Based on this prerequisite, we not only approximate a driver's speed adjustment for car following in the next subsection but also summarise some important properties revealed in the phase of quantum transformation of visual stimuli which are presented as follows.

**Property 1 (The effects of visual stimuli):** Given that a vehicle (the target vehicle) remains moving in a lane without traffic intervention from other lanes, the instantaneous attention allocation range ( $\Delta x(t)$ ) in the longitudinal dimension of the target driver is negatively affected by aggregate psychophysical momentum ( $\Phi_{J_Q}(t)$ ) derived from the perceived surrounding traffic flows in the following forms:

(1-a) *Given  $W_i(t)$ ,  $m_{j_Q}$ ,  $\forall j_Q \in J_Q$  and external environmental conditions, as the perceived aggregate relative speed of the surrounding traffic flow moving toward the target vehicle increases, the instantaneous visual spread ( $\Delta x(t)$ ) of the target driver in the longitudinal dimension decreases, contributing to the increase in target driver attention on the object nearest the focal point, and vice versa.*

A typical example is the case in which the target vehicle approaches the tail of queuing vehicles in a traffic bottleneck from the light traffic segment to the heavy traffic segment on a freeway. The target driver typically pays close attention to the front vehicle in the same lane when first perceiving queuing vehicles. Another case is when the target vehicle approaches a lane-blocking incident from an adjacent lane in which incident-induced queuing vehicles stuck in the blocked lane may contribute a certain amount of visual stimuli perceived by the target driver even in the absence of any front vehicle in an adjacent lane. This case also infers the necessity of car-following model extension in rationalising incident-induced lane traffic phenomena.

(1-b) *Given  $W_i(t)$ ,  $\Delta v_{j_Q \rightarrow i}(t)$ ,  $\forall j_Q \in J_Q$ , and external environmental conditions, as the perceived aggregate light mass of the surrounding traffic flow increases, the instantaneous visual spread ( $\Delta x(t)$ ) of the target driver in the longitudinal dimension decreases, thereby contributing to the increase in the attention of the target driver on the object nearest the focal point, and vice versa.*

In reality, this sub-property can be easily observed when comparing two different cases in which a truck and car moving ahead are observed, respectively, given the same moving

speed and traffic flow conditions. According to the proposed model, the perception of a truck may result in more visual stimuli than a car, thereby receiving more attention from the target driver. This issue, however, appears to be sparsely addressed in the previous literature of car-following behaviour modelling.

(1-c) *Given  $m_{j_Q}$ ,  $\Delta v_{j_Q \rightarrow i}(t)$ ,  $\forall j_Q \in J_Q$ , and external environmental conditions, as the size of attentional resources ( $W_i(t)$ ) of the target driver increases, the instantaneous visual spread ( $\Delta x(t)$ ) of the target driver in the longitudinal dimension decreases, thereby contributing to the increase in the attention the target driver pays to the object nearest the focal point, and vice versa.*

This sub-property can be easily induced from Equation (14). The greater the target driver's attentional resources ( $W_i(t)$ ) the smaller the instantaneous visual spread ( $\Delta x(t)$ ) of the driver in the longitudinal dimension given  $m_{j_Q}$  and  $\Delta v_{j_Q \rightarrow i}(t)$  ( $\forall j_Q \in J_Q$ ), thus increasing the driver's attention allocated on the object nearest the focal point. In effect, this sub-property is arguably reasonable, and consistent with the principle of the zoom-lens model proposed by Eriksen and St James (1986) in the area of selective visual attention. Therein, the change in size of focus is deemed to have a trade-off relationship with the efficiency of processing in the visual field.

## 2.2. Approximation of speed adjustment

This phase describes a quantum-mechanics-based approach for reproducing a driver's speed adjustment during the car-following process driven by psychological stimuli (i.e. psychophysical momentums ( $\Phi_{j_Q}(t)$ )). Based on the aforementioned prerequisite (i.e.  $[\Delta v_{j_Q \rightarrow i}(t)] \rightarrow [v_{j_Q \rightarrow i}(t)]$ ), the surrounding traffic flow conditions perceived by a driver were transformed into driver psychophysical momentums ( $\Phi_{j_Q}(t)$ ) in the previous phase. In this phase, psychophysical momentums are further processed through a stochastic wave packet procedure to characterise the quantum-based optical effect on target driver attention, and then are correlated with the induced speed adjustment. The developmental procedures are described as follows.

First, by adopting the theorems of Beiser (1969) and Morrison (1990), this work characterises the attention of the target driver in the instantaneous visual field  $Q[\Delta x(t), \Delta y(t)]$  using a two-dimensional Gaussian wave packet ( $\Omega_{Q[\Delta x(t), \Delta y(t)]}[x(t), y(t)]$ ) in the following generalised form:

$$\Omega_{Q[\Delta x(t), \Delta y(t)]}[x(t), y(t)] = \frac{e^{-\frac{1}{2} \left[ \frac{[x(t) - \mu_{Q_x}(t)]^2}{(\Delta x(t))^2} + \frac{[y(t) - \mu_{Q_y}(t)]^2}{(\Delta y(t))^2} \right]}}{2\pi \times \Delta x(t) \times \Delta y(t)} \quad (18)$$

where  $\mu_{Q_x}(t)$  and  $\mu_{Q_y}(t)$  are the centres of the instantaneous wave packet in the  $X$ - and  $Y$ -dimensions, respectively. The instantaneous psychophysical momentum ( $\Phi_{j_Q}(t)$ ) induced by each surrounding vehicle ( $j_Q$ ,  $\forall j_Q \in J_Q$ ) is then associated with a time-varying weight ( $\delta_{i,j_Q}(t)$ ) given by

$$\delta_{i,j_F}(t) = \frac{\Omega_{Q[\Delta x(t), \Delta y(t)]}[x_{j_Q}(t), y_{j_Q}(t)]}{\sum_{\forall j'_Q \in J_Q} \Omega_{Q[\Delta x(t), \Delta y(t)]}[x_{j'_Q}(t), y_{j'_Q}(t)]}, \quad \forall j_Q \in J_Q \quad (19)$$

where  $\delta_{i,j_Q}(t)$  also represents the relative magnitude of the attention of the target driver on a given perceived vehicle  $j_Q$  at time  $t$ .

Accordingly, one can utilise the above two-dimensional Gaussian wave packet ( $\Omega_{Q[\Delta x(t), \Delta y(t)]}[x(t), y(t)]$ ) to aggregate the psychophysical momentums ( $\Phi_{j_Q}(t)$ ) of the target driver perceived within  $Q[\Delta x(t), \Delta y(t)]$ . The resulting response of the target driver can then be treated as the speed adjustment ( $\dot{v}_i(t + \Delta t_i)$ ) of the target vehicle at time  $t + \Delta t_i$ , as determined by the sum of weighted psychophysical momentums resulting from perceived vehicles dispersing ahead. The mathematical form of  $\dot{v}_i(t + \Delta t_i)$  is given by

$$\begin{aligned}\dot{v}_i(t + \Delta t_i) &= \alpha_1 \times \Phi_{j_Q}(t) \\ &= \alpha_1 \times \sum_{\forall j_Q \in J_Q} \delta_{i,j_Q}(t) \times \Phi_{j_Q}(t) \\ &= \alpha_1 \times W_i(t) \times \sum_{\forall j_Q \in J_Q} \delta_{i,j_Q}(t) \times [m_{j_Q} \times v_{j_Q \rightarrow i}(t)]\end{aligned}\quad (20)$$

where  $\alpha_1$  is a positive parameter, and  $\Delta t_i$  is the reaction time of target driver  $i$ .

The rationales of the proposed quantum optical-flow-based driver stimulus-response model derived above are now discussed.

First, the proposed model is particularly applicable during lane-blocking incidents. Empirically, during a lane-blocking incident, any vehicle approaching the incident site from either a blocked lane or adjacent lanes may not adjust their speeds based merely on the behaviour of the front vehicle. Instead, drivers typically adapt their approaching speeds to an aggregate speed of the incident-impacted traffic flows moving ahead that are responding to incident effects on section-wide traffic flows (Sheu *et al.* 2001, Sheu 2003). In reality, when using the proposed model, the incident effect on section-wide traffic flows can be characterised by driver-perceived multi-vehicle momentum to derive driver responses to incident-induced traffic phenomena. Such a treatment appears to be more realistic in dealing with incident-induced driver behaviour.

Second, from a psychophysical perspective, that the magnitude of the speed adjustment by the target vehicle also relies on the size of driver attentional resources ( $W_i(t)$ ) is reasonable. Theoretically, a driver with a large value of  $W_i(t)$  may have increased awareness of surrounding traffic situations (Endsley 1995, Recarte and Nunes 2002). This may contribute to increased deceleration when negative changes in surrounding traffic situations are perceived (e.g. surrounding traffic worsens, and approaches a lane-drop segment). Conversely, a driver with fewer attentional resources ( $W_i(t)$ ) can be less sensitive to the same traffic situations. Therefore,  $W_i(t)$  is proportional to the speed adjustment, as in Equation (20). Additionally, from a practical perspective, such a psychological factor can be further characterised through sophisticated mechanisms to reproduce microscopic traffic behaviour. For example, it is likely that a driver's visual attention can be influenced by other uncertainties, e.g. instantaneous driving workloads (Hing *et al.* 2003, Jahn *et al.* 2005), emotions (Lajunen *et al.* 1998) and familiarity degree in route conditions (Martens and Fox 2007), and moreover, may decline with the length of driving time due to fatigue. And thus, the factor of attentional resources ( $W_i(t)$ ) can be determined via stochastic processes with decreasing mean values over time and diverse variances, and then incorporated into traffic simulators to characterise the heterogeneity of driver visual attention in traffic simulation. With respect to the instantaneous measurement of  $W_i(t)$  for potential use in ITS subsystems such as advanced vehicle control and safety systems

(AVCSS) and automatic highway systems (AHS), the utilisation of other advanced psychophysical technologies for measuring a driver's activation and arousal conditions is needed.

Third, consider two cases associated with two different front vehicles (e.g. a truck and a private vehicle) perceived by the target driver. The resulting magnitude of the speed adjustment by the target driver can differ in these two cases. Intuitively, a target driver is likely to pay more attention when approaching a truck than when approaching a private vehicle due to psychological discomfort and safety concerns (Yoo and Green 1999, Peeta *et al.* 2005, de Waard *et al.* 2008), thereby resulting in different speed adjustments for these two cases. Notably, such vehicle effects during car following can also be differentiated via the use of psychophysical momentum in the proposed model; and however, may not be satisfactorily addressed by existing car-following models.

Additionally, some properties of the proposed model revealed in this phase are summarised as follows.

**Property 2 (Relationships between visual stimuli and driving response):** Given that a vehicle (the target vehicle) remains in a lane without traffic intervention from other lanes, the speed adjustment ( $\dot{v}_i(t + \Delta t_i)$ ) and aggregate psychophysical momentum ( $\Phi_{J_Q}(t)$ ) of the target driver based on perceived surrounding traffic flows have a causal relationship.

(2-a) *Given  $W_i(t)$ ,  $v_{j_Q \rightarrow i}(t)$ ,  $\forall j_Q \in J_Q$ , and external environmental conditions, as the perceived aggregate mass of surrounding vehicles increases, the attention the target driver pays to the front vehicle in the same lane increases, contributing to the phenomenon in that the speed adjustment ( $\dot{v}_i(t + \Delta t_i)$ ) of the target driver relies markedly on the behaviour of the front vehicle, and vice versa.*

Under high-volume traffic conditions, a target driver may perceive a greater magnitude of aggregate light mass ( $\mathbf{M}_{J_Q}(t)$ ) than that when under low-volume traffic conditions. This may further increase the attention the target driver pays to the object nearest the focal point, i.e. the front vehicle (by sub-property 1-b), and decrease  $\Delta x(t)$  and  $\Delta y(t)$  in  $\Omega_{Q[\Delta x(t), \Delta y(t)]}[x(t), y(t)]$  (see Equation (18)).

Furthermore, sub-property 2-a also indicates that from a psychophysical perspective, speed adjustment manoeuvres reproduced in the existing car-following literature are special cases addressed by the proposed model. That is, under the condition of multi-lane over-congestion or only one vehicle moving ahead in the same lane, the proposed model may generate results similar to those generated by existing car-following models. Nevertheless, in most cases, driver intra-lane speed adjustment manoeuvres may still be influenced by aggregate psychophysical momentum in response to the perception of multi-lane traffic flow situations, according to the proposed quantum optical-flow-based model.

(2-b) *Given  $W_i(t)$ ,  $m_{j_Q}(t)$ ,  $\forall j_Q \in J_Q$ , and external environmental conditions, as the perceived aggregate relative speed of the surrounding traffic flow moving toward the target vehicle increases (i.e.  $\sum_{\forall j_Q \in J_Q} \delta_{i,j_Q}(t) \times [m_{j_Q} \times v_{j_Q \rightarrow i}(t)] < 0$ ), the degree to which target driver deceleration ( $\dot{v}_i(t + \Delta t_i) < 0$ ) relies on the behaviour of the front vehicle moving in the same lane increases, and vice versa.*

Sub-property 2-b has two important features. First, the directional correlation between perceived relative speed and the resulting speed adjustment ( $\dot{v}_i(t + \Delta t_i)$ ) of the target vehicle is consistent with outcomes yielded by existing car-following models. For instance, given that only one front vehicle  $j_Q$  is ahead and the perceived relative speed is negative

(i.e.  $v_{j_Q \rightarrow i}(t) < 0$ ), target vehicle  $i$  may decelerate, in accordance with Equation (19). Specifically, as the perceived deceleration increases, the resulting deceleration of the target vehicle increases. Second, this sub-property particularly applies to the case in which the target vehicle is approaching a highly congested segment upstream from a segment with a low degree of congestion. Due to the quantum optical flow effect in sub-property 1-a, the target driver may increase his attention on the front vehicle as the aggregate speed at which the perceived surrounding traffic flow is moving backward is significant in this case. If the perceived relative speed is extremely high, the magnitude of target vehicle deceleration will depend on the behaviour of the front vehicle, mimicking classical car-following phenomena.

(2-c) *Given  $m_{j_Q}$ ,  $v_{j_Q \rightarrow i}(t)$ ,  $\forall j_Q \in J_Q$ , and external environmental conditions, as the attentional resources ( $W_i(t)$ ) of the target driver increase, the sensitivity of the target driver to the behaviour of the front vehicle increases, and thus the target driver typically executes a greater speed adjustment after perceiving the speed adjustment of the front vehicle, compared with that for fewer attentional resources.*

Based on the proposed model and properties, this work now considers their applicability to various traffic scenarios.

#### Scenario 1: One target vehicle following one front vehicle

This work now considers a simple car-following scenario, in which two successive vehicles, the target and front vehicle (denoted by  $i$  and  $j_Q$ ), are moving at speeds  $v_i(t)$  and  $v_{j_Q}(t)$ , respectively, in a given lane on a road segment without changing lanes. From Equations (1) and (2), the peripheral visual field  $Q[\Delta x(t), \Delta y(t)]$  of the target vehicle is formed with instantaneous visual spreads  $\Delta x(t)$  and  $\Delta y(t)$  in the longitudinal ( $X$ ) and lateral ( $Y$ ) dimensions, respectively. In this car-following scenario, the target driver perceives the front vehicle in the focal point located in  $(\frac{\Delta x(t)}{2}, 0)$  relative to the position of the target driver. According to Equation (20), we infer that the instantaneous speed adjustment  $v_i(t + \Delta t_i)$  of the target driver is

$$\begin{aligned}\dot{v}_i(t + \Delta t_i) &= \alpha_1 \times \Phi_{j_Q}(t) \\ &= \alpha_1 \times W_i(t) \times \delta_{i,j_Q}(t) \times m_{j_Q} \times v_{j_Q \rightarrow i}(t) \\ &= \alpha_1 \times W_i(t) \times \delta_{i,j_Q}(t) \times m_{j_Q} \times [v_{j_Q}(t) - v_i(t)]\end{aligned}\quad (21)$$

By Equation (19),  $\delta_{i,j_Q}(t) = 1$ , which is applied to Equation (21); thus,  $v_i(t + \Delta t_i)$  is given by

$$\dot{v}_i(t + \Delta t_i) = \alpha_1 \times W_i(t) \times m_{j_Q} \times [v_{j_Q}(t) - v_i(t)] \quad (22)$$

For this simple car-following scenario, the derived model in Equations (21) and (22) has properties similar in reality that are the generalised form of the GHR model (i.e.  $\dot{v}_i(t + \Delta t_i) = \beta(v_i(t))^b \frac{v_{j_Q}(t) - v_i(t)}{[x_{j_Q}(t) - x_i(t)]^a}$ ), which has been extensively investigated in car-following and related areas in traffic flow theory (Brackstone and McDonald 1999). First, the proposed quantum-mechanics-based model and GHR model have a common feature in which the perceived relative speed of the target vehicle, i.e.  $v_{j_Q}(t) - v_i(t)$ , has a direct linear effect on the speed adjustment ( $v_i(t + \Delta t_i)$ ), where  $v_i(t + \Delta t_i)$  increases as  $v_{j_Q}(t) - v_i(t)$  increases.

Second, consider the effect of the relative position on  $v_i(t + \Delta t_i)$  in both models. As stated, the front vehicle is perceived in the focal point of the target driver at time  $t$  and, thus,

$$\begin{aligned} \frac{\Delta x(t)}{2} &= x_{j_Q}(t) - x_i(t) \\ \Rightarrow \Delta x(t) &= 2[x_{j_Q}(t) - x_i(t)] \end{aligned} \quad (23)$$

By combining Equations (12) and (23), we infer that as the magnitude of the relative position  $x_{j_Q}(t) - x_i(t)$  decreases, the psychophysical momentum  $\Phi_{j_Q}(t)$  of the target driver increases. Thus, according to Equation (21), the magnitude of the speed adjustment  $v_i(t + \Delta t_i)$  increases. We infer that the effect of  $x_{j_Q}(t) - x_i(t)$  on  $v_i(t + \Delta t_i)$  in the proposed quantum-mechanics-based model is similar to that in the GHR car-following model. Moreover, in both the models, the instantaneous speed ( $v_i(t)$ ) of the target vehicle has a positive effect on the speed adjustment  $v_i(t + \Delta t_i)$  of the target vehicle driver. By Equation (22), we infer that the effect of  $v_i(t)$  on  $v_i(t + \Delta t_i)$  in the GHR model can be rationalised by utilising  $W_i(t)$  in the proposed model.

Accordingly, the typical car-following behaviour reproduced by GHR-based models can be considered a special case characterised in the proposed quantum optical-flow-based model. Specifically, the proposed model remains valid when differentiating type-of-vehicle effects on  $v_i(t + \Delta t_i)$  under conditions when front vehicles are different types due to the incorporation of  $m_{j_Q}$  in the proposed model.

#### Scenario 2: Rubbernecking-driven car-following when passing incidents

This scenario demonstrates the applicability of the proposed model in characterising potential driving behaviour of the target driver while perceiving a lane-blocking incident in an adjacent lane. Unlike the previous incident-free scenario, the curiosity of the target driver regarding the perceived incident and anomalous changes in section-wide traffic flows, particularly in terms of queuing upstream of the incident site, may result in the so-called rubbernecking effect on car following when the target vehicle approaches the incident. Specifically, the incident-induced rubbernecking car-following behaviour stems from the diversion of target driver attention from perceived traffic flows spreading towards the incident site, coupled with personal driving pressure that may increase when approaching the incident site from an adjacent lane. Such mixed psychological factors contribute to incident-induced rubbernecking car-following behaviour that may go beyond classical car-following logic rules in, say, the GHR-based model.

To characterise incident-induced rubbernecking in the car-following model, the derived quantum-based model (Equation (20)) can be rewritten as

$$\begin{aligned} \dot{v}_i(t + \Delta t_i) &= \alpha_1 \times \Phi_{j_Q}(t) \\ &= \alpha_1 \times \{\Phi_{i-1}(t) + \Phi_{\Lambda}(t) + \Phi_{j_{\Lambda}}(t)\} \\ &= \alpha_1 \times W_i(t) \times \left\{ \delta_{i,i-1}(t) \times [m_{i-1} \times v_{i-1 \rightarrow i}(t)] + \delta_{i,\Lambda}(t) \times [m_{\Lambda} \times v_{\Lambda \rightarrow i}(t)] \right. \\ &\quad \left. + \sum_{\forall j_{\Lambda} \in J_Q} \delta_{j_{\Lambda}}(t) \times m_{j_{\Lambda}} \times v_{j_{\Lambda} \rightarrow i}(t) \right\} \\ &= \alpha_1 \times W_i(t) \times \left\{ \delta_{i,i-1}(t) \times [m_{i-1} \times v_{i-1 \rightarrow i}(t)] - \delta_{i,\Lambda}(t) \times m_{\Lambda} \times v_i(t) \right. \\ &\quad \left. + \sum_{\forall j_{\Lambda} \in J_Q} \delta_{j_{\Lambda}}(t) \times m_{j_{\Lambda}} \times v_{j_{\Lambda} \rightarrow i}(t) \right\} \end{aligned} \quad (24)$$

Equation (24) suggests that when approaching an incident site from an adjacent lane, three main sources of psychophysical momentums exist, i.e.  $\Phi_{i-1}(t)$ ,  $\Phi_{\Lambda}(t)$  and  $\Phi_{j_{\Lambda}}(t)$ , each of which influence target driver speed adjustment ( $v_i(t + \Delta t_i)$ ). Thus,  $\Phi_{i-1}(t)$ ,  $\Phi_{\Lambda}(t)$  and  $\Phi_{j_{\Lambda}}(t)$  represent the psychophysical momentums caused by the perceived front vehicle ( $i - 1$ ) in the same lane, the incident ( $\Lambda$ ) and incident-affected vehicles ( $\forall j_{\Lambda}$ ) upstream from  $\Lambda$  in the blocked lane, respectively. Similarly, the values of the corresponding time-varying weights  $\delta_{i,i-1}(t)$ ,  $\delta_{i,\Lambda}(t)$  and  $\delta_{i,j_{\Lambda}}(t)$  can be approximated using Equations (18) and (19). According to Equation (24), we infer that in the presence of a lane-blocking incident, the instantaneous speed adjustment ( $v_i(t + \Delta t_i)$ ) of the target driver may rely on the perceived manoeuvres of the front vehicle, the effect of personal attention diversion on the perceived incident event and the affected vehicles upstream from the incident site in blocked lanes. Notably, such an inference is not found in car-following literature.

Based on Equation (24), this work now considers the following incident-induced car-following phenomena that are sparsely addressed in existing car-following models.

First, the front vehicle  $i - 1$  is downstream of the incident site and moving with an instantaneous speed of  $v_{i-1}(t)$ , where  $v_{i-1}(t) > v_i(t)$ . Some vehicles are perceived as queued in the blocked lane upstream of incident  $\Lambda$ , as illustrated in Phenomenon (1) (Figure 2). By applying classical car-following rules (e.g. GHR-based models) to this phenomenon, a positive speed adjustment of the target vehicle can be derived, i.e.  $v_i(t + \Delta t_i) > 0$ , which may not be absolutely correct in real cases due to the influence of the aforementioned psychological factors affecting the behaviour of the target driver. The proposed model, however, yields the following proposition:

**Proposition 1:** *Given a lane-blocking incident with a certain number of vehicles queuing in the blocked lane, and the perceived acceleration (i.e.  $v_{i-1}(t) > v_i(t)$ ) of the front vehicle, the*

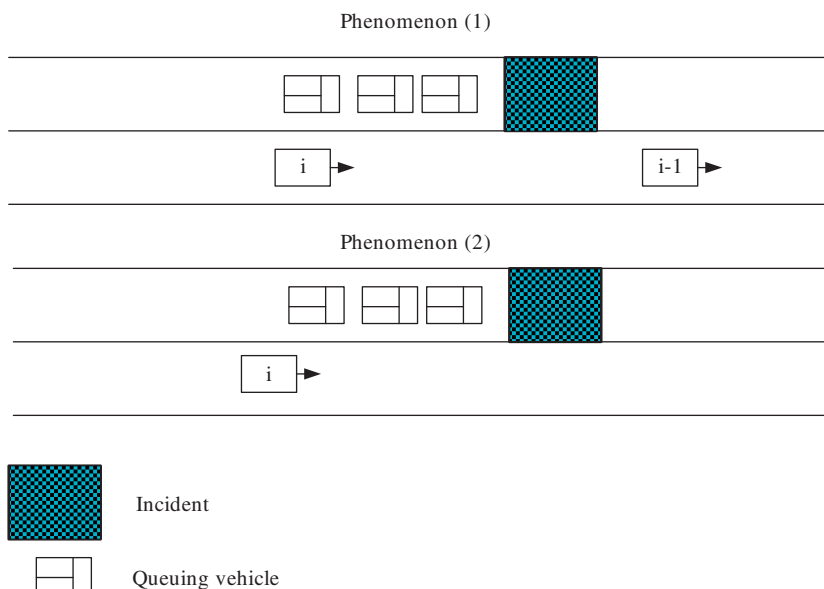


Figure 2. Illustration of incident-induced lane traffic phenomena.

target driver will accelerate (i.e.,  $v_i(t + \Delta t_i) > 0$ ) only when Equation (20) holds. Otherwise, the target driver typically maintains the same speed or decelerates (i.e.  $v_i(t + \Delta t_i) \leq 0$ ) when passing the incident site.

$$\delta_{i,i-1}(t) \times m_{i-1} \times v_{i-1}(t) > \left[ \delta_{i,i-1}(t) \times m_{i-1} + \delta_{i,\Lambda}(t) \times m_{\Lambda} + \sum_{\forall j_{\Lambda} \in J_Q} \delta_{j_{\Lambda}}(t) \times m_{j_{\Lambda}} \right] \times v_i(t) \quad (25)$$

**Proof:** According to Equation (24),  $v_i(t + \Delta t_i) > 0$  only when

$$\begin{aligned} & \alpha_1 \times \Phi_{J_Q}(t) > 0 \\ & \Rightarrow \Phi_{i-1}(t) + \Phi_{\Lambda}(t) + \Phi_{j_{\Lambda}}(t) > 0 \quad (\because \alpha_1 > 0) \\ & \Rightarrow \delta_{i,i-1}(t) \times [m_{i-1} \times v_{i-1 \rightarrow i}(t)] + \delta_{i,\Lambda}(t) \times [m_{\Lambda} \times v_{\Lambda \rightarrow i}(t)] \\ & \quad + \sum_{\forall j_{\Lambda} \in J_Q} \delta_{j_{\Lambda}}(t) \times m_{j_{\Lambda}} \times v_{j_{\Lambda} \rightarrow i}(t) > 0 \quad (\because W_i(t) > 0) \\ & \Rightarrow \delta_{i,i-1}(t) \times [m_{i-1} \times (v_{i-1}(t) - v_i(t))] > \delta_{i,\Lambda}(t) \times m_{\Lambda} \times v_i(t) \\ & \quad + \sum_{\forall j_{\Lambda} \in J_Q} \delta_{j_{\Lambda}}(t) \times m_{j_{\Lambda}} \times v_i(t) \quad (\because v_{j_{\Lambda}}(t) = 0, \quad \forall j_{\Lambda}) \\ & \Rightarrow \delta_{i,i-1}(t) \times m_{i-1} \times v_{i-1}(t) > \left[ \delta_{i,i-1}(t) \times m_{i-1} + \delta_{i,\Lambda}(t) \times m_{\Lambda} + \sum_{\forall j_{\Lambda} \in J_Q} \delta_{j_{\Lambda}}(t) \times m_{j_{\Lambda}} \right] \times v_i(t) \end{aligned} \quad (26)$$

Thus, Proposition 1 is proved.

Notably, Proposition 1 also applies to the case in which no queuing vehicles are perceived in the blocked lane. In this case, the necessary condition (i.e. Equation (25)) becomes

$$\delta_{i,i-1}(t) \times m_{i-1} \times v_{i-1}(t) > [\delta_{i,i-1}(t) \times m_{i-1} + \delta_{i,\Lambda}(t) \times m_{\Lambda}] \times v_i(t) \quad (27)$$

If we assume  $m_{i-1} = m_{\Lambda}$ , this condition can be simplified as

$$\delta_{i,i-1}(t) \times v_{i-1}(t) > [\delta_{i,i-1}(t) + \delta_{i,\Lambda}(t)] \times v_i(t) \quad (28)$$

If we assume that the mass of the perceived incident object (e.g. a broken vehicle) is the same as the mass of the front vehicle ( $m_{i-1} = m_{\Lambda}$ ), and, moreover, the target driver pays full attention to the front vehicle (i.e.  $\delta_{i-1} = 1$ ,  $\delta_{i,\Lambda} = 0$ ) while passing an incident, the above condition (Equation (28)) may be redundant. Thus, the behaviour of the target driver in Proposition 1 holds true unconditionally. In other words, given the aforementioned scenario, the proposed model may reproduce the typical car-following behaviour characterised by existing car-following models. Again, this implies that the car-following behaviour reproduced by classical models is merely the result of a special case characterised by the proposed model.

Next, consider another incident-induced lane traffic phenomenon, i.e. Phenomenon (2) (Figure 2), in which a certain number of vehicles are queuing in a blocked lane, and only

one vehicle (i.e. the target vehicle) is approaching the incident site from the target lane (i.e. the lane adjacent to the blocked lane). Using classical car-following rules may result in an impractical projection when there is no front vehicle ahead of the target vehicle in this case because typical ‘car-following refers to a situation in which a vehicle’s speed and longitudinal position are influenced by the vehicle immediately ahead of it in the same travel lane’ (Ranney 1999). Conversely, due to the optical stimulus caused by perceiving these queued vehicles, the speed adjustment ( $v_i(t + \Delta t_i)$ ) of the target driver derived from the proposed quantum optical flow-based car-following model (Equation (24)) is

$$\dot{v}_i(t + \Delta t_i) = -\alpha_1 \times W_i(t) \times v_i(t) \times \left[ \delta_{i,\Lambda}(t) \times m_\Lambda + \sum_{\forall j_\Lambda \in J_Q} \delta_{j_\Lambda}(t) \times m_{j_\Lambda} \right] \quad (29)$$

Notably, Equation (29) reveals several generalisations. First, under a perceived lane-blocking incident in an adjacent lane, the target driver typically decelerates, i.e.  $v_i(t + \Delta t_i) < 0$ , even when no front vehicle is present. Second, the magnitude of deceleration by the target driver in this case depends mainly on the size of driver attentional resources ( $W_i(t)$ ), approaching speed ( $v_i(t)$ ), the perceived aggregated mass of the incident ( $m_\Lambda$ ) and queuing vehicles ( $m_{j_\Lambda}$ ,  $\forall j_\Lambda$ ). Specifically, as the number of queued vehicles perceived by the target driver increases, deceleration by the target driver increases, thereby amplifying the negative effect of the incident on road capacity, which is consistent with findings by Sheu (2003) and Sheu *et al.* (2004). Notably, even when no vehicle is queuing upstream of an incident site, according to Equation (29) the incident effect still exists, and, thus, leads to target driver deceleration by

$$\dot{v}_i(t + \Delta t_i) = -\alpha_1 \times W_i(t) \times v_i(t) \times \delta_{i,\Lambda}(t) \times m_\Lambda \quad (30)$$

This is why a lane-blocking incident always results in time-varying negative effects on road traffic performance from a microscopic perspective.

Furthermore, since the instantaneous psychophysical momentum ( $\Phi_{i-1}(t)$ ) in Equation (24) is directional, it can contribute to the corresponding speed adjustment of the target driver (positive or negative), which depends on perceived relative speed ( $\Delta v_{i-1 \rightarrow i}(t)$ ). Conversely, the second term in Equation (24) is not a directional quantity; thus, it contributes to a purely negative effect on speed adjustment in the equation. Accordingly, the two extreme cases discussed above demonstrate the applicability of the proposed model for incident cases in relation to conventional car-following theories.

Overall, the proposed model may characterise how a driver adjusts vehicular speed in a lane in response to perceived multi-lane traffic flow situations. The typical car-following behaviour characterised in literature can be regarded as a special case in which the driver of the following vehicle pays full attention to the front vehicle in the same lane.

### 3. Preliminary tests and results

Considering the prototype of the proposed methodology, this work aimed at preliminary tests to reveal the potential of the model’s applicability in car-following behaviour characterisation at the current stage. Furthermore, to demonstrate the model’s transferability, two test scenarios associated with two different datasets collected at different study sites were utilised in the tests: (1) video-based processed dataset collected on an N-3 urban

highway in Taiwan and (2) NGSIM video-based processed dataset collected on southbound 101 freeway in California. Evaluation measures were based mainly on comparisons of the speed adjust values (i.e. acceleration/deceleration) outputted from the proposed model and video-based processed data. Test procedures and results in these two scenarios are described respectively in the following.

The study site of the first test scenario (Test scenario-1) was a 1-km two-lane segment of N-3 urban highway located in southern Taiwan, where two cameras were installed, one on the upstream and one on the downstream sections of the study site to videotape lane traffic movement. The average traffic volume at the study site was about 784 vehicles/ln/h, and average speed was 56.2 km/h, based on the collected video-based data. In this test scenario, three probe vehicles, the target, front, and experimental control (EC) vehicles were used; the target and front vehicles were deployed in the outside lane, and the EC-vehicle was in the inner lane (Figure 3). The instantaneous speeds of the target and front vehicles were recorded using in-vehicle cameras, and the perceived movements of surrounding vehicles were videotaped from the viewpoint of the target driver.

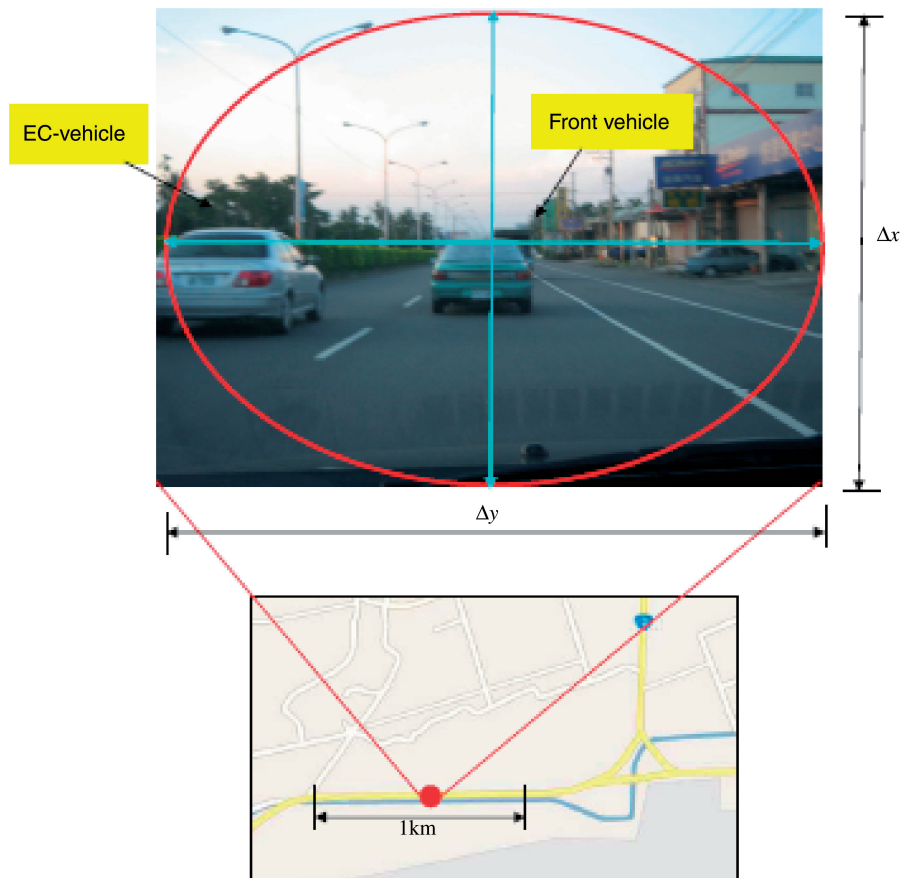


Figure 3. Allocation of probe vehicles at the 1st study site.

Conversely, the EC-vehicle, which was deployed in the adjacent lane, moved at different experimental speeds in the range of 10–70 km/h with an incremental speed of 10 km/h to generate diverse traffic flow conditions. Particularly, we designed a low-speed experimental case in which the EC-vehicle kept moving very slowly (10–30 km/hr) with a flash alarm at the rear of the vehicle for safety. The sampling period for each dataset was 3 min, covering the time at which the probe vehicles enter and exit the study site.

In this test scenario, a total of 14 video-based raw datasets were generated, where each raw dataset contains 1 s. microscopic data samples, including the instantaneous speeds and locations associated with these probe vehicles. Based on the 1 s raw data samples, we generated 180 data samples for each dataset with respect to target vehicle's speed adjustment during the 3 min sampling period. Among the 14 video-based datasets, five were utilised to calibrate the parameter of  $\alpha_1$  (see Equation (20)) which was set to be 0.308 in this test scenario. Note that the driver attentional-resource term ( $W_i(t)$ ) hinges on the internal properties of a driver, as mentioned previously. As only one target vehicle was considered in this test scenario, we normalised the value of  $W_i(t)$ , and assumed it to be one ( $W_i(t) = 1$ ) for simplicity meaning that the target driver's visual attention is fully allocated on the perceived traffic situations at the 1 km study site. The rest of the nine datasets were then used to test the performance of the proposed model.

To evaluate the model's performance in reproducing car-following behaviour, two types of measures: (1) comparisons of average link travel time of target vehicles and (2) distributions of absolute values of relative prediction errors were adopted. The corresponding test results obtained in this test scenario are presented in Table 1 and Figure 4. A discussion of the test results is presented in the following.

Overall, the above test results indicate the acceptability of the proposed quantum optical flow-based approach in reproducing car-following behaviour, which can be explicated in two aspects. First, by comparing the predicted values with video-based data with respect to average link travel time, we can infer that the proposed model's capability of characterising vehicular speed adjustment in a car-following process is reasonably accepted. As revealed in Table 1, the target vehicle's link travel time forecasted using the proposed model is close to the video-based data as the relative prediction errors are lower than 10% in all three experimental cases. Note that in this test scenario, the target vehicle was requested to keep moving in a given lane throughout the study site without considering lane changing behaviour. That is, the target driver was allowed to adjust

Table 1. Comparisons of average link travel time of target vehicles (Test scenario 1).

Data source measurement	Video-based data (s)	Proposed model (s)	Relative prediction error (%)
Case-1: EC-vehicle with high speed (50–70 kph)			
Link travel time of target vehicle	57.2	60.4	5.59
Case-2: EC-vehicle with medium speed (30–50 kph)			
Link travel time of target vehicle	63.3	66.8	7.11
Case-3: EC-vehicle with low speed (10–30 kph)			
Link travel time of target vehicle	74.6	81.1	8.71
Overall performance	65.0	69.1	6.31

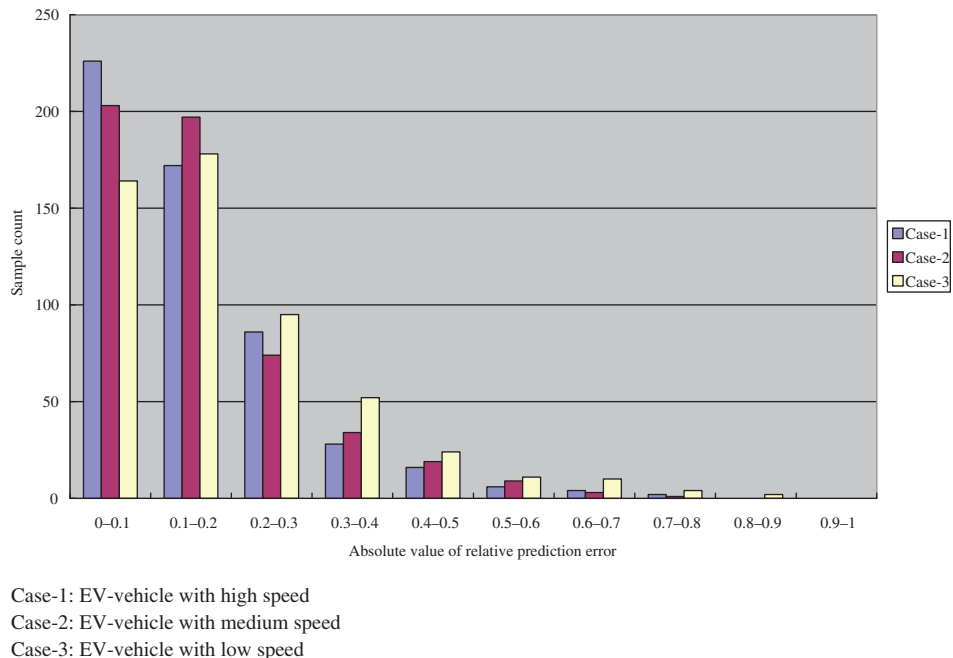


Figure 4. Distribution of absolute values of relative prediction errors (Test scenario 1).

vehicular speed only for the purpose of car following. Therefore, the resulting link travel time of the target vehicle can also be regarded as an index to assess the proposed model's performance in reproducing microscopic car-following behaviour. Second, Figure 4 reveals that most of the prediction errors with respect to speed adjustments are distributed within the range  $-0.2$  to  $0.2$ , and such a convergence of forecast errors also implies that the proposed model's forecast performance is reliable over time.

Additionally, we had also noted that the relative prediction errors associated with the experimental case-3 (i.e. EV-vehicle with low speed) appeared to disperse more widely than the other two cases (Figure 4). According to our observation, this phenomenon can be a mixed effect caused by the high variance in speed perception of the target driver at lower speeds and lane-changing interference from the adjacent lane (where the low-speed EC-vehicle moves). We observed that in the experimental case-3, the EC-vehicle moving with an extremely low speed (10–30 km/h) had resulted in the slowdowns of the following vehicles which might be forced to conduct lane-changing from the adjacent lane to the target lane (i.e. the lane the target vehicle moves on). In this study case, such a lane-changing fraction (from the adjacent lane) was about 0.78 encountered by the target driver while approaching the low-speed EC-vehicle. Consequently, the target vehicle was usually forced to slow down while passing by the low-speed EC-vehicle due to the lane-changing interference from the adjacent lane. Meanwhile, the target driver's lateral field might become wider at such lower speeds, thus leading to high variance in speed perception, according to quantum optical flow theory (Baker 1999). Accordingly, we also reason that the proposed quantum optical flow-based car-following model may suffer more challenges

under high congestion conditions (particularly in lane-blocking incidents), and thus must rely on integration with other microscopic traffic behaviour models (Sheu 2008).

To demonstrate the proposed model's capability of reproducing car-following behaviour with glancing-around effect, this work sampled three typical vehicular spatiotemporal trajectories drawn from video-based data and simulation data yielded with and without the glancing-around effect on car following outputted from the proposed model. Simulation output without the influence of glancing around was obtained by assuming drivers pay full attention to front vehicles in the same lane during car following; thus, the time-varying weight ( $\delta_{i,i-1}(t)$ ) is set to 1. Figure 5 shows the graphical comparison result with respect to vehicular spatiotemporal trajectory (i.e. vehicular moving distance associated with time) present in a lane. The vehicular spatiotemporal trajectories with the glancing-around effect are more congruent with video-based data than those obtained without the glancing-around effect. This is also the reason why overall performance of the proposed model for intra-lane microscopic traffic characterisation in tests is acceptable.

The second study site (Test scenario-2) was located on a 6-lane segment of U.S. Highway 101 (i.e. Hollywood Freeway) in Los Angeles, California. In this test scenario, we sampled the vehicles shown in the 101 dataset videotaped from 08:20am to 08:35am on 15 June 2005 by camera 4, where the camera field was 75 m in length, covering the longitudinal domain of the southbound segment of the study site (Figure 6). The hourly volume was about 1390 vehicles/in/h and average speed was about 33.2 km/h at the study site. Therein, short-term traffic jams with queuing vehicles, followed by shockwave phenomena were occasionally observed during the 15 min sampling period. Vehicles were classified into three types: (1) motorcycles, (2) automobiles and (3) trucks and buses, accounting for 0.3%, 97.6% and 2.1%, respectively, according to the summary report by Cambridge Systematics Inc. (2005). The complete NGSIM video-based datasets are open to the public, and can be accessed via <http://ngsim-community.org/>.

In this test scenario, we aimed at the car-following behaviour of vehicles present in the middle lane (the 3rd inside lane). A total of 178 vehicles were sampled to generate 1 s processed dataset. For each sampled vehicle (termed the target vehicle), we recorded the vehicle types, vehicular trajectories and link travel time, and then calculated relative speeds associated with these target vehicle and perceived surrounding vehicles for each second until the target vehicle disappeared from the camera field.

Based on the above recorded data, we generated 1296, 1 s data samples with respect to target vehicles' speed adjustments in this scenario. Therein, we used the generated 583 data samples (associated with 78 sampled vehicles) to calibrate the parameter of  $\alpha_1$  which was set to be 0.287 in this test scenario, and the rest of the 713 data samples (associated with 100 sampled vehicles) for model tests. Differing from the previous test scenario in which only one target driver was considered, there were 178 target drivers present in this test scenario. Therefore, we assumed that  $W_i(t)$  associated with each target vehicle follows a uniform distribution bounded by 0.5 and 1, and then adopted the corresponding random number generated from the uniform distribution for the estimation of  $\alpha_1$  and model tests.

Similarly, the two assessment measures adopted in Test scenario-1 are used in this test scenario (Test scenario 2). The corresponding test results obtained in this test scenario are shown in Table 2 and Figure 7. In addition, vehicular spatiotemporal trajectories of lane-3 drawn from video-based data and prediction data using the proposed model are also presented in Figure 8 for comparison. An overall discussion of test results is presented below.

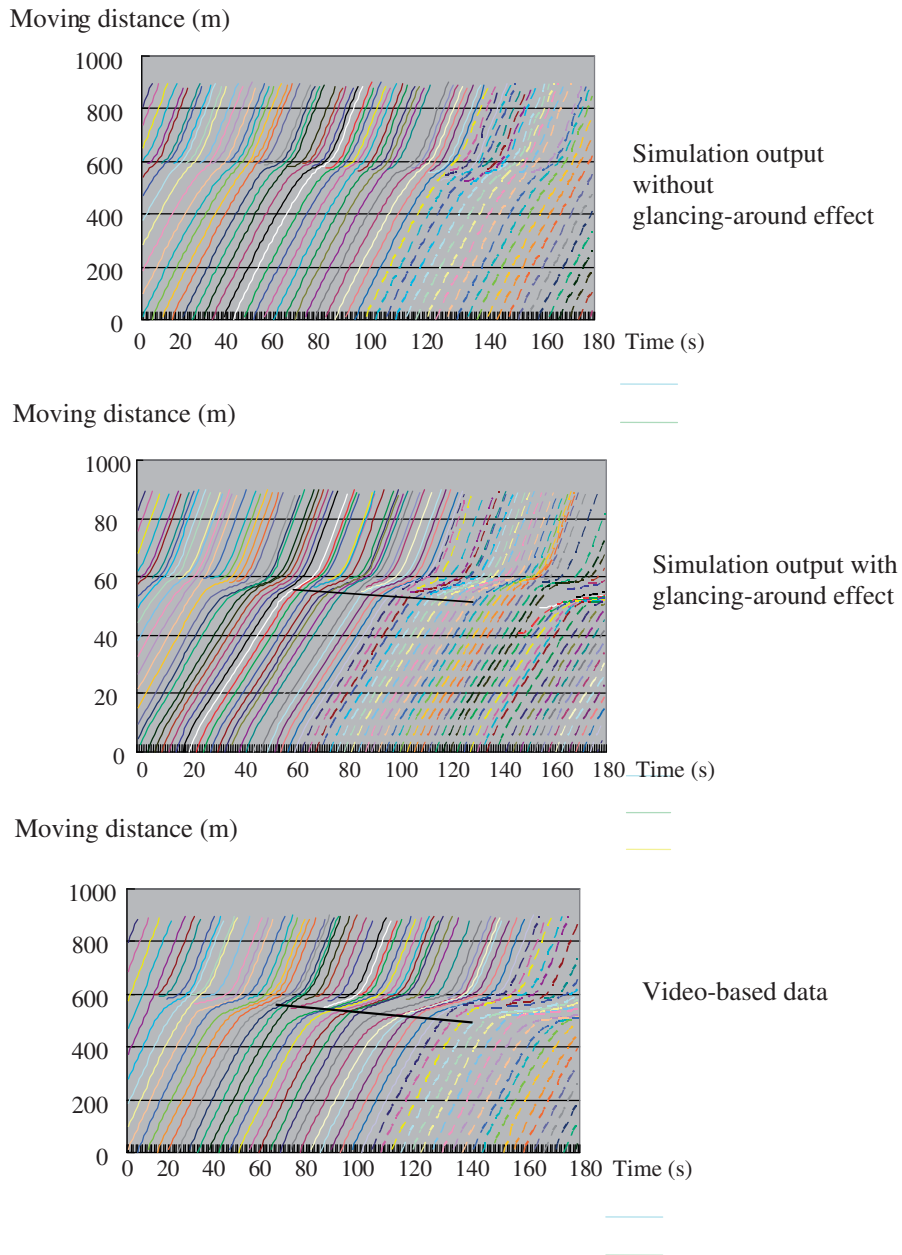


Figure 5. Samples of vehicular spatiotemporal trajectories (Test scenario-1).

Overall, the above test results also indicate the acceptability of the proposed quantum optical flow-based approach in reproducing car-following behaviour on freeways, particularly under medium- and high-volume traffic flow conditions. Relative to the 1st study site, traffic is more congested at the 2nd study site with the average

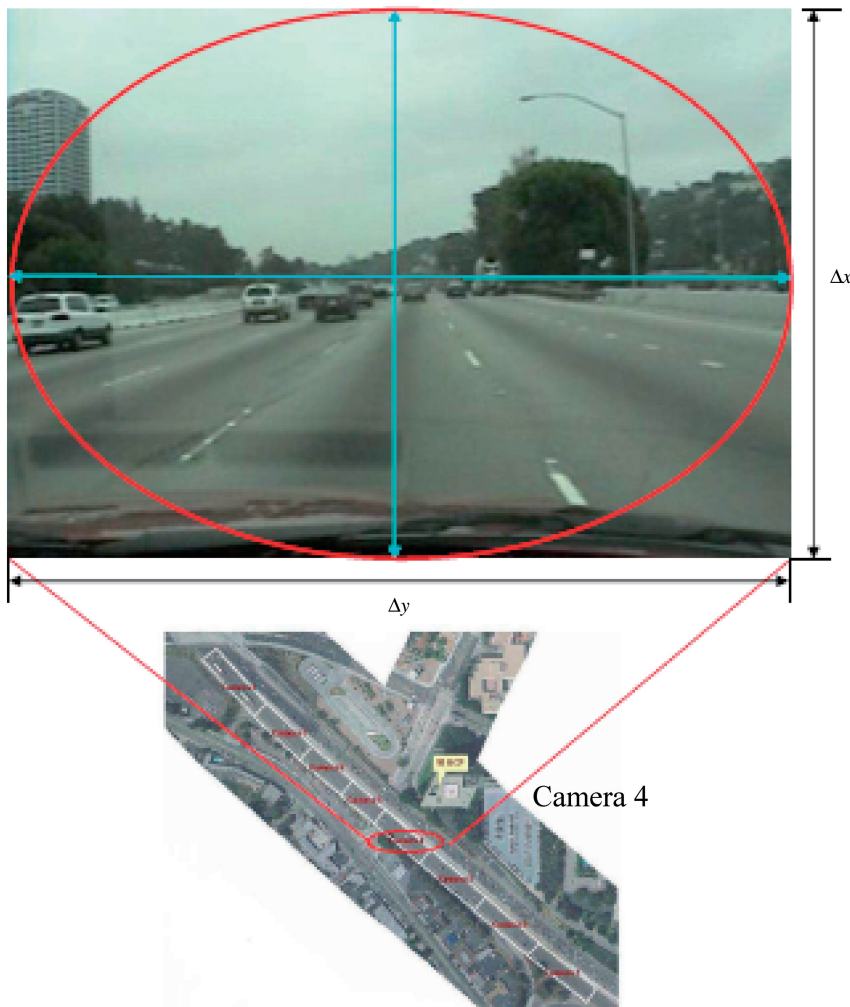


Figure 6. 2nd study site (Test scenario-2).

Source: NGSIM 101 dataset (by Cambridge Systematic Inc., 2005).

Table 2. Comparison of average link travel time (Test scenario 2).

Comparison of averaged link travel time

Data source	Measurement	Video-based data (s)	Proposed model (s)	Relative prediction error (%)
Averaged link travel time		7.8	8.5	8.97

speed 33.2 km/h, which is lower than that at the 1st study site (56.2 km/h). Nevertheless, the comparison of the results of average link travel time is accepted because the relative prediction error (0.0897) is less than 0.1 (Table 2). Additionally, Figure 7 also shows good correspondence between the predicted speed adjustments and video-based data, thus

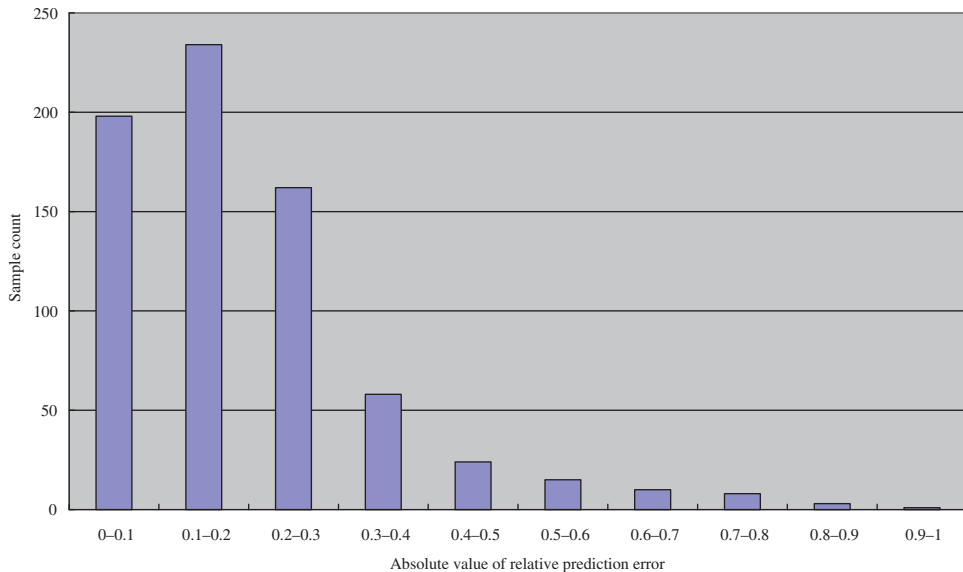


Figure 7. Distribution of absolute values of relative prediction errors (Test scenario 2).

resulting in the congruence of predicted vehicular trajectories with real ones observed from video. In reality, the test results obtained in this scenario may be encouraging to those researchers (like us) who would like to bridge the gap between quantum optical flow theory and microscopic traffic behaviour modelling. We have also noted some early works (e.g. Baker 1999) which claim that the quantum uncertainty relationship may hold only under high speed conditions. Therein, we infer that the feasibility of quantum optical flow theory in the characterisation of microscopic traffic behaviour at low speeds must hinge on some indispensable conditions. More specifically, we claim that a constrained speed-perception error condition (e.g.  $[\Delta v_{J_Q \rightarrow i}(t)] \rightarrow [v_{J_Q \rightarrow i}(t)]$  assumed in this work) is indispensable to improve the rationality of quantum uncertainty relationship in approximating a driver's speed adjustment for car-following at a low speed. Additionally, we had also noted that the distribution with respect to relative prediction errors shown in Figure 7 is not as concentrated as seen in the previous test scenario (Figure 4). Such a phenomenon, in reality, is not surprising as the previous evidence had shown that the lower the physical speed, the higher the speed perception error (Baker 1999).

On the other hand, we argue that the treatment of either the size of attentional resources ( $W_i(t)$ ) or reaction time ( $\Delta t_i$ ) can be another issue in model tests and applications. Unlike the previous literature in quantum optical flow theory which aims at the quantum uncertainty relationship characterised in the focal point of a person, the proposed model deals with generalised car-following behaviour attributed to a variety of drivers on roadways. However, the aforementioned two human factors may vary with driver characteristics (e.g. age, sex and instantaneous psychophysical conditions) and external situational conditions (Hing *et al.* 2003). For instance, we assumed  $\Delta t_i$  to be a constant (set to be 0.91) in this study. However, the vehicular trajectories observed under high-congestion conditions (Figure 8) revealed that personal reaction time occurring in the

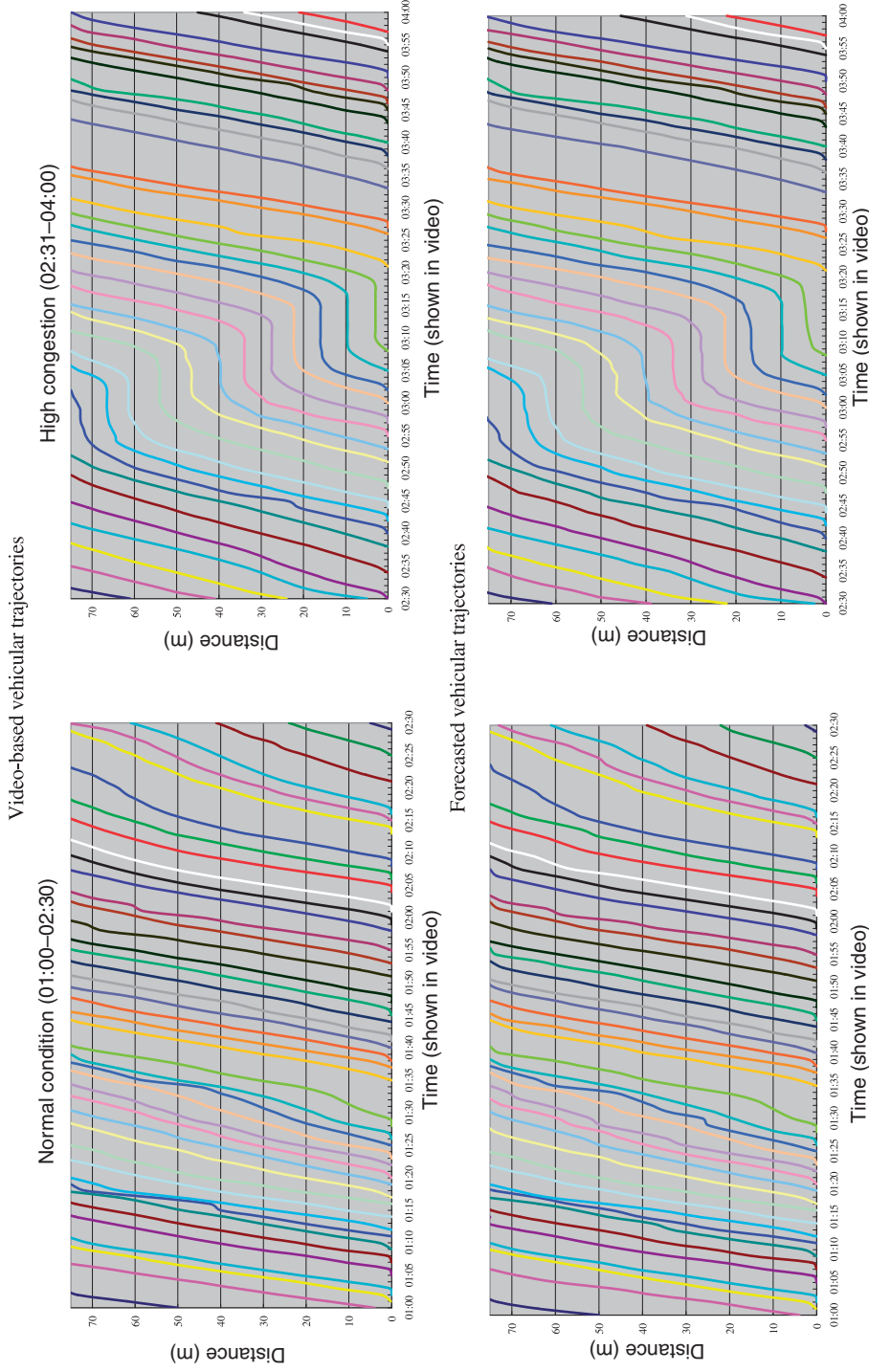


Figure 8. Samples of vehicular spatiotemporal trajectories (Test scenario-2).

start-up process (during a forward shockwave) appeared to vary with drivers, and a little longer than that occurring in the braking process (during a backward shockwave). Such uncertainty in reaction time observed during a forward shockwave (i.e. when vehicular queuing starts to disperse) may contribute to irregular start-up delays, thus leading to greater deviations in reproducing vehicular trajectories, compared with normal car-following cases. More specifically, we speculate that the joint uncertainty in  $\Delta t_i$  and  $W_i(t)$  may exist, and collectively influence quantum optical field and driver behaviour. Briefly, the characterisation of these human factors with more elaborate measures warrants more investigation.

Moreover, based on analytical results the following provides some insights on the size of attentional resources ( $W_i(t)$ ) to facilitate determination of  $W_i(t)$  for further applications of the proposed model.

- (1) Theoretically, the size of attentional resources reflecting the degree of a person's physiological arousal with respect to a perceived object may vary with fluctuations in physical and physical situations, age, and task conditions (Hasher and Zacks 1979, Humphreys and Revelle 1984, Young and Stanton 2002). Nevertheless, most applied research on attention has implicitly assumed it to be fixed for simplification in applications (Wickens 1984, Wickens and Hollands 2000). Accordingly, we adopt a fixed value used to quantify  $W_i(t)$  in the 1st test scenario, and however, a random number drawn from a given distribution in the 2nd test scenario to reflect the heterogeneity of target drivers for preliminary tests. Such a simplification in determination of  $W_i(t)$  seems to be arguably agreeable in this work, according to the previous literature.
- (2) Evidence showing that attentional resources may shrink to accommodate any mental demand reduction is accumulating (Young and Stanton 1997, 1999, 2001, 2002), inferring that a lower level of  $W_i(t)$  can be set for low-volume traffic flow cases than that set for high-volume cases for practical applications.
- (3) Although there is no consensus with respect to the measurement of  $W_i(t)$  in the field of attention theory, it seems widely agreeable that visual gaze reflects attention allocation (Underwood and Everatt 1996). Thus, any technologies that can measure the proportion of time spent in looking at target objects can be used for the measurement of  $W_i(t)$  for practical applications. For instance, in the experiment designed by Young and Staton (2002), attentional gaze was measured utilising an onboard miniature camera directed at an experimental participant's face. The video-based data were then used to investigate attentional resources hypotheses.

Additionally, some other lane traffic phenomena that are challenging for the use of quantum optical flow theory in driver behaviour modelling have also been noticed. First, inter-lane traffic phenomena such as lane changes from adjacent lanes caused by unusual events (e.g. anomalous slowdown of the experimental control vehicle in Test scenario 1 to mimic lane-blocking incidents) markedly influence the wave-image duality and speed perception of a driver, leading to more complexity in characterising the quantum optical flow of a driver while car following. Furthermore, lane-changing effects may vary over time and space, as well as instantaneous traffic flow conditions. Additionally, the experimental design did not aim to test the proposed model under various lane-changing

scenarios such as incident-induced lane changes and lane drops, thus leaving room for more experiments.

#### 4. Conclusions and recommendations

This work rationalised the dynamics of the driver stimulus-response process during car following using a novel quantum-mechanics-based psychophysical methodology. To consider the potential effects of driver perceptions of surrounding traffic situations, a novel quantum optical-flow-based approach incorporating driver psychophysical momentum, which is determined by several psychophysical factors (e.g. driver attentional resources and the perception of surrounding traffic flow conditions), is incorporated into the proposed model. Then, a microscopic traffic behaviour module, which consists of stimulus and response phases, is designed to approximate driver speed adjustments during car following under the perception of surrounding traffic situations. Furthermore, several generalisations provide further insights into intra-lane microscopic traffic phenomena.

Preliminary test results reveal that the proposed model permits reproducing car-following behaviour using the quantum-mechanics-based methodology. Notably, the proposition that driver intra-lane speed adjustment is influenced by the perceived surrounding traffic dynamics underlying the proposed model was proved by qualitative and quantitative analyses. Based on these generalisations from analytical results, typical car-following behaviour reproduced by existing models may be a unique phenomenon in which the following driver allocates all attention to the front vehicle at all times. Thus, this is a special case characterised by the proposed model. Moreover, the proposed method can approximate driver speed adjustment under the glancing-around effect in response to perceived anomalous traffic flows in adjacent lanes. This may also rationalise the incident-induced lane traffic phenomenon in that all multi-lane traffic flows upstream from an incident site unexpectedly slowdown in most lane-blocking incident cases.

Nevertheless, additional effort in data collection and a relatively more complex experimental design using advanced devices is needed to verify the validity of the proposed model. Further tests for urban street cases are also suggested such that more influential factors, such as traffic signals and inference from turning movement and roadside parking, can be examined. Furthermore, additional effort in determination of the size of driver attentional resources and examination of the influence of driver visual attention on the performance of the proposed model is also needed. Incorporating other technologies and approaches (e.g. fuzzy theory) to approximate driver psychophysical momentum, particularly in terms of the perceived light mass and relative speed of surrounding traffic, also warrants further research. Deriving induced lane traffic flow phenomena by extending the proposed model and analytical results is also a worthwhile task. In addition to the development of advanced traffic simulators, future research through model extension and integration with image processing technologies for the use in ITS subsystems such as AVCSS and AHS is also suggested. Most importantly, this work elucidates the influence of human psychological and physical factors on driving manoeuvres to improve road safety, and will stimulate further investigations exploring issues and solutions to add to literature on traffic flow theory.

## References

Baker, R.G.V., 1999. On the quantum mechanics of optic flow and its application to driving in uncertain environments. *Transportation Research Part F*, 2, 27–53.

Bartmann, D., Spijker, W., and Hess, M., 1991. Street environment, driving speed and field of vision. In: A.G. Gale, I.D. Brown, C.M. Haslegrave, I. Moorhead, and S.P. Taylor, eds. *Vision in vehicle III*. Amsterdam: Elsevier, 381–389.

Beiser, A., 1969. *Perspectives of modern physics*. New York: McGraw-Hill.

Brackstone, M. and McDonald, M., 1999. Car-following: a historical review. *Transportation Research Part F*, 2, 181–196.

Cambridge Systematics Inc., 2005. NGSIM US 101 dataset analysis (08:20am to 08:35am), Summary Report prepared for Federal Highway Administration, December 2005. <http://www.camsys.com>.

Cavallo, V. and Laurent, M., 1988. Visual information and skill level in time-to-collision estimation. *Perception*, 17, 623–632.

Chakraborty, P. and Kikuchi, S., 1999. Evaluation of the general motors based car-following models and a proposed fuzzy inference model. *Transportation Research C*, 7C (4), 209–235.

Chandler, R.E., Herman, R., and Montroll, E.W., 1958. Traffic dynamics: studies in car following. *Operations Research*, 6, 165–184.

Davis, L.C., 2003. Modification of the optimal velocity traffic model to include delay due to driver reaction time. *Physica A*, 319, 557–567.

de Waard, D., Kruizinga, A., and Brookhuis, K.A., 2008. The consequences of an increase in heavy goods vehicles for passenger car drivers' mental workload and behaviour: a simulator study. *Accident Analysis and Prevention*, 40, 818–828.

Endsley, M.R., 1995. Toward a theory of situation awareness in dynamic systems. *Human Factors*, 37 (1), 32–64.

Eriksen, C. and St James, J., 1986. Visual attention within and around the field of focal attention: a zoom lens model. *Perception and Psychophysics*, 40 (4), 225–240.

Fodor, J.A., 1983. *The modularity of mind*. Cambridge, MA: The MIT Press.

Fritzsche, H.-T., 1994. A model for traffic simulation. *Transportation Engineering Contribution*, 5, 317–321.

Gazis, D.C., Herman, R., and Rothery, R.W., 1961. Nonlinear following-the-leader models of traffic flow. *Operations Research*, 9, 545–567.

Gibson, J.J., 1966. *The senses considered as a perceptual system*. Boston: Houghton Mifflin.

Gong, H., Liu, H., and Wang, B.-H., 2008. An asymmetric full velocity difference car-following model. *Physica A*, 387, 2595–2602.

Hasher, L. and Zacks, R.T., 1979. Automatic and effortful processes in memory. *Journal of Experimental Psychology: General*, 108, 356–388.

Herman, R. and Rothery, R.W., 1965. Propagation of disturbances in vehicular platoons. In: L. Edie, R. Herman, and R.W. Rothery, eds. *Vehicular traffic science*. New York: American Elsevier, 14–25.

Hing, J.Y.C., Stamatiadis, N., and Aultman-Hall, L., 2003. Evaluating the impact of passengers on the safety of older drivers. *Journal of Safety Research*, 34 (4), 343–351.

Humphreys, M.S. and Revelle, W., 1984. Personality, motivation, and performance: a theory of the relationship between individual differences and information processing. *Psychological review*, 91, 153–184.

Jahn, G., et al., 2005. Peripheral detection as a workload measure in driving: effects of traffic complexity and route guidance system use in a driving study. *Transportation Research Part F*, 8, 255–275.

Jiang, R. and Wu, Q.-S., 2007. The night driving behavior in a car-following model. *Physica A*, 375, 297–306.

Kahneman, D., 1973. *Attention and effort*. Englewood Cliffs, NJ: Prentice-Hall.

Kayser, H.J. and Hess, M., 1991. The dependency of drivers' viewing behavior on speed and street environment structure. In: A.G. Gale, I.D. Brown, C.M. Haslegrave, I. Moorhead, and S.P. Taylor, eds. *Version in vehicles III*. Amsterdam: Elsevier, 89–94.

Kikuchi, S. and Chakroborty, P., 1992. Car-following model based on fuzzy inference system. *Transportation Research Record*, 1365, 82–91.

Lajunen, T., Parker, D., and Stradling, S.G., 1998. Dimensions of driver anger, aggressive, and highway code violations and their mediation by safety orientation in UK drivers. *Transportation Research Part F*, 1, 107–121.

Lee, D.N., 1980. The optic flow field: the foundation of vision. *Philosophical Transactions of the Royal Society*, 290, 169–179.

MacLeod, R.W. and Ross, H.E., 1983. Optic flow and cognitive factors in time-to-collision estimates. *Perception*, 12, 417–423.

Martens, M.H. and Fox, M.R.J., 2007. Do familiarity and expectations change perception? Drivers' glances and response to changes. *Transportation Research Part F*, 10, 476–492.

May, A.D., 1990. *Traffic flow fundamentals*. Englewood Cliffs, NJ: Prentice-Hall.

Miura, T., 1987. Behavior oriented version: functional field of view and processing resources. In: J.K. O'Regan, and A. Levy-Schoen, eds. *Eye movements: from physiology to cognition*. Amsterdam: Elsevier, 563–572.

Morrison, M.A., 1990. *Understanding quantum physics: a user manual*. New Jersey: Prentice-Hall.

Newell, G.F., 1961. Nonlinear effects in the dynamics car following. *Operations Research*, 9, 209–229.

Orosz, G., Krauskopf, B. and Wilson, R., 2005. Bifurcations and multiple traffic jams in a car-following model with reaction time delay. *Physica D* 211, 277–293.

Osaka, N., 1988. Speed estimation through restricted visual field. In: A.G. Gale, M.H. Freeman, C.M. Haslegrave, P. Smith, and S.P. Taylor, eds. *Version in vehicles II*. Amsterdam: Elsevier, 45–55.

Panwai, S. and Dia, H., 2005. Comparative evaluation of microscopic car-following behaviour. *IEEE Transactions on Intelligent Transportation Systems*, 6 (3), 314–325.

Patten, C.J.D., et al., 2004. Using mobile telephones: cognitive workload and attention resource allocation. *Accident Analysis and Prevention*, 36, 341–350.

Peeta, S., Zhang, P., and Zhou, W., 2005. Behavior-based analysis of freeway car-truck interactions and related mitigation strategies. *Transportation Research Part B*, 39, 417–451.

Pipes, L.A., 1953. An operational analysis of traffic dynamics. *Journal of Applied Physics*, 24 (3), 274–281.

Ranney, T.A., 1999. Psychological factors that influence car-following and car-following model development. *Transportation Research Part F*, 2, 213–219.

Recarte, M.A. and Nunes, L., 2002. Mental load and loss of control over speed in real driving toward a theory of attentional speed control. *Transportation Research Part F*, 5, 111–122.

Sheu, J.-B., 2008. A quantum mechanics-based approach to model incident-induced dynamic driver behavior. *Physica D*, 237, 1800–1814.

Sheu, J.-B., Chou, Y.-H., and Chen, A., 2004. Stochastic modeling and real-time prediction of incident effects on surface street traffic congestion. *Applied Mathematical Modelling*, 28 (5), 445–468.

Sheu, J.-B., 2003. A stochastic modeling approach to real-time prediction of queue overflows. *Transportation Science*, 37 (1), 97–119.

Sheu, J.-B., Chou, Y.-H., and Shen, L.-J., 2001. A stochastic estimation approach to real-time prediction of incident effects on freeway traffic congestion. *Transportation Research-Part B*, 35B (6), 575–592.

Tampere, C.M., Hoogendoorn, S.P., and van Arem, B., 2009. Continuous traffic flow modeling of driver support systems in multiclass traffic with intervehicle communication and drivers in the loop. *IEEE Transactions on Intelligent Transportation Systems*, 10 (4), 649–657.

Underwood, G. and Everatt, J., 1996. Automatic and controlled information processing: the role of attention in the processing of novelty. *In: O. Neumann, and A.F. Sanders, eds. Handbook of perception and action.* London: Academic, 185–227.

Wickens, C.D., 1984. Processing resources in attention. *In: R. Parasuraman, and R. Davies, eds. Varieties of attention.* New york: Academic, 63–101.

Wickens, C.D. and Hollands, J.G., 2000. *Engineering psychology and human performance.* 3rd ed. Upper Saddle River, NJ: Prentice Hall.

Wiedemann, R., 1991. Modelling of RTI-elements on multi-lane roads. In the Commission of the European Community, Advanced Telematics in Road Transport, Vol. DG XIII.

Yoo, H., and Green, P., 1999. Driver behavior while following cars, trucks, and buses. Project report prepared for University of Michigan Transportation Research Institute, UMTRI-99-14, Ann Arbor, MI.

Young, M.S. and Stanton, N.A., 2002. Malleable attentional resources theory: a new explanation for the effects of mental underload on performance. *Human Factors: The Journal of Human Factors and Ergonomics Society*, 44, 365–375.

Young, M.S. and Stanton, N.A., 2001. Size matters: the role of attentional capacity in explaining the effects of mental under-load on performance. *In: D. Harris, ed. Engineering psychology and cognitive ergonomics: Volume 5, aerospace and transportation systems.* Aldershot, UK: Ashgate, 357–364.

Young, M.S. and Stanton, N.A., 1999. Miles away: a new explanation for the effects of automation on performance. *In: M.A. Hanson, E.J. Lovesey, and S.A. Robertson, eds. Contemporary ergonomics, 1999.* London: Taylor and Francis, 73–77.

Young, M.S. and Stanton, N.A., 1997. Automotive automation: investigating the impact on driver's mental workload. *International Journal of Cognitive Ergonomics*, 1, 325–336.